

Grafting Monodisperse Polymer Chains from Concave Surfaces of Ordered Mesoporous Silicas

Michal Kruk,^{*,†,§} Bruno Dufour,^{†,||} Ewa B. Celer,^{‡,⊥} Tomasz Kowalewski,[†] Mietek Jaroniec,[‡] and Krzysztof Matyjaszewski^{*,†}

Department of Chemistry, Carnegie Mellon University, Pittsburgh, Pennsylvania 15213, and Kent State University, Kent, Ohio 44242

Received July 21, 2008; Revised Manuscript Received September 2, 2008

ABSTRACT: Surface-initiated atom transfer radical polymerization (ATRP) was used to graft uniform layers of polyacrylonitrile (PAN), poly(2-(dimethylamino)ethyl methacrylate), and polystyrene on concave surfaces of cylindrical mesopores of diameter ~ 10 nm and spherical mesopores of diameter ~ 15 nm. The grafting process was optimized through the introduction of appropriate amounts of Cu(II) species that act as a deactivator, allowing us to grow polymer layers of controlled thickness (as seen from gas adsorption), which consisted of monodisperse polymer chains of controlled molecular weight (as seen from gel permeation chromatography). For PAN, the degrees of polymerization ranged from $DP = 25$ to 70 , and the polydispersity indexes of the polymer grafted under optimal conditions were as low as $M_w/M_n = 1.06$ – 1.07 . Grafted chain densities up to 0.28 chains/nm² and initiation efficiencies up to 37% were achieved. In cases of spherical mesopores of diameter ~ 15 nm, it was possible to introduce significant loadings of polymer (up to 28 wt % in resulting composite) without making the uniform mesopores inaccessible. The specific surface areas of the silica/polymer hybrids were 70 – 350 m² g⁻¹, and the thicknesses of the polymer films were controlled in the range up to 1 – 2 nm without causing any major pore blockage. This work demonstrates new opportunities in the synthesis of well-defined nanostructured/nanoporous silica/polymer hybrids.

Introduction

The synthesis of polymers in well-defined nanoporous media has been an exciting area of research that has implications on fields of electronics,^{1–4} polymer synthesis,^{5–7} controlled release,⁸ and heterogeneous catalysis.⁹ The functionalization of surfaces of nanoporous materials with well-defined polymers^{9–12} is a new frontier in the development of porous inorganic–organic hybrid materials with designed properties. Because of the diversity of structural and functional properties of polymers, the modification of solid surfaces with polymers can be viewed as perhaps the most robust approach for the surface functionalization with organic moieties, rendering desired hydrophobic/hydrophilic properties, chemical stability, catalytic properties, stimuli-responsive properties, and so forth.^{13–19} One of the approaches explored recently was the polymerization of vinyl monomers and appropriate cross-linkers on the surface of mesopores (pores of diameter between 2 and 50 nm²⁰) and in the micropores (pores of diameter below 2 nm²⁰) of ordered mesoporous silicas (SBA-15 with cylindrical pores) with complementary microporosity.⁹ The polymer formed in micropores served as an anchor for the polymer layer on the surface of mesopores. In cases of supports with appropriate complementary microporosity, an excellent control of the thickness of the cross-linked polymer film was demonstrated, and the blockage of the pores with polymer was avoided. SBA-15 was also used as support for the introduction of thin layers of polyaniline either through adsorption of monomer from vapor phase²¹ or copolymerization of surface-bonded monomer with

monomer in solution.²² The growth of dendrimers in well-defined pores of high-surface-area silicas has recently been demonstrated.^{23,24}

Another emerging opportunity in the introduction of well-defined polymer species on surfaces of porous materials is related to the development of surface-initiated controlled polymerization methods, which allow one to form polymer brushes, that is, high-surface-density layers of well-defined polymer chains covalently bonded to solid support.^{25–31} Atom transfer radical polymerization (ATRP)^{32–35} is particularly convenient as a means for the controlled growth of polymers initiated from solid surfaces,^{11,25,27,29,31,36–44} but other controlled radical polymerization methods were also successfully used.^{28,45–47} Surface-initiated ATRP was explored^{11,27,48} for macroporous materials (pore diameter above 50 nm²⁰) that exhibit specific surface areas of ~ 10 – 100 m² g⁻¹. In some cases, the grafted polymer had a narrow molecular weight distribution.²⁷ The growth of polymer chains in cylindrical pores of anodic alumina (diameter 20 – 200 nm)⁴⁹ or in voids between the spheres of diameter ~ 200 nm in colloidal crystals were also explored,^{50,51} but no information about the polydispersity of the polymer graft and, in the first case,⁴⁹ about the accessibility of pores after polymerization was reported. The surface-initiated ATRP was used to graft poly(*N*-isopropylacrylamide) (PNIPAAm) on the surface of cylindrical mesopores of diameter ~ 3 nm,⁵² but taking into account that prior to the polymerization the pore diameter was decreased by the introduction of a layer of the initiation sites, the resulting pore diameter would be sufficient to accommodate only one or several polymer chains. Similarly, the grafting of polystyrene in cylindrical pores (diameter ~ 3 nm) of MCM-41 was attempted via nitroxide-mediated polymerization (NMP),⁵³ but the resulting silica/polymer composite exhibited the specific surface area of only 20 m² g⁻¹, and no evidence of pore accessibility was provided. More recently, external surfaces of MCM-41 particles were grafted with PNIPAAm⁵⁴ and poly(methyl methacrylate) (PMMA).⁵⁵

* Corresponding authors: e-mail kruk@mail.csi.cuny.edu, tel (718) 982 4030, fax (718) 982 3910 (M.K.); e-mail km3b@andrew.cmu.edu, tel (412) 268 3209, fax (412) 268 6897 or (412) 268 1061 (K.M.).

[†] Carnegie Mellon University.

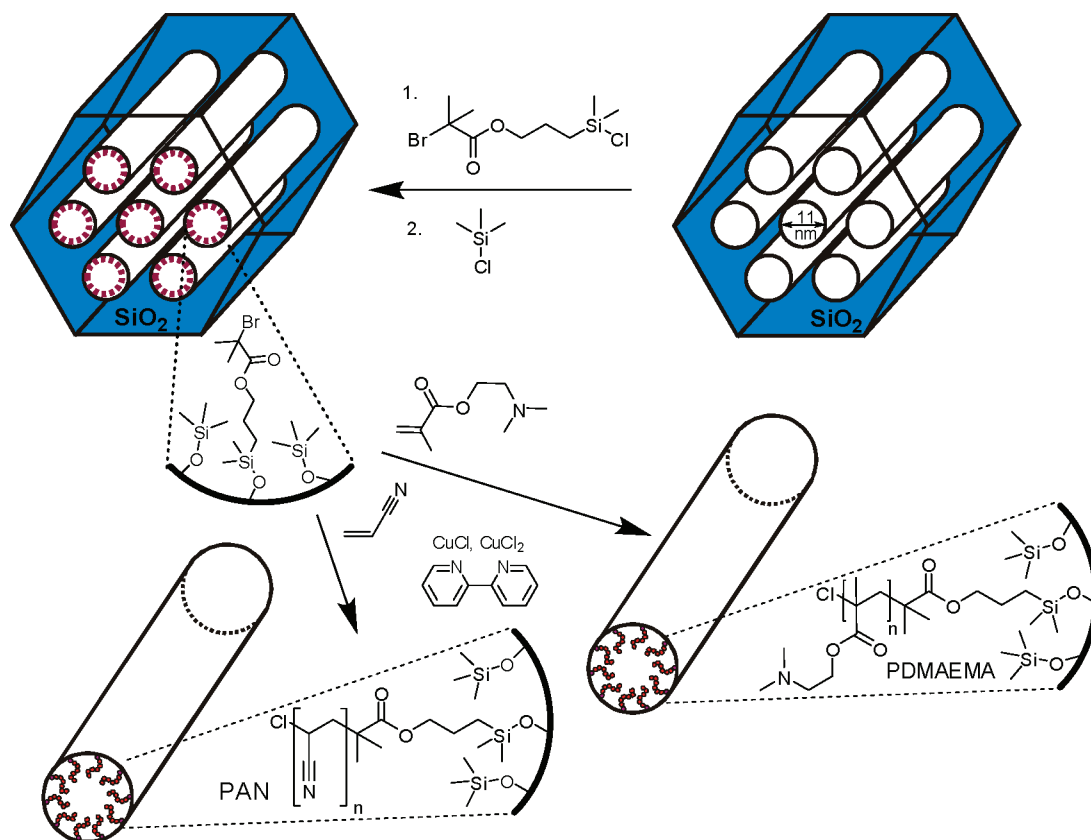
[‡] Kent State University.

[§] Present address: Department of Chemistry, College of Staten Island and Graduate Center, City University of New York, Staten Island, NY 10314.

^{||} Present address: Corning SAS, Avon, France.

[⊥] Present address: Quantachrome Instruments, Boyton Beach, FL 33426.

Scheme 1. Surface-Initiated Atom Transfer Radical Polymerization in Ordered Nanopores



Recently, the research on grafting of polymers from high-surface-area materials with pores of diameter 5–50 nm has begun to attract much attention. We demonstrated that ATRP can be used to grow uniform polymer layers on the surfaces of mesopores of chromatographic silica gels (nominal pore diameter ~20 and 50 nm).^{56,57} In most cases, the pores were accessible after polymerization, and the amount of grafted polymer increased with the polymerization time. Later, PNIPAAm was grafted from the surface of relatively large spherical pores (diameter 22 nm) of silica mesocellular foam using ATRP initiator,⁵⁸ but a moderate amount of polymer was introduced and the reported gas adsorption data indicated unexpected formation of large pores after the introduction of the polymer, pointing to a complex nature of the polymer grafting procedure. We used the surface-initiated ATRP to completely fill the cylindrical pores of ordered mesoporous silica SBA-15⁵⁹ (diameter ~10 nm) and spherical pores of FDU-1 (diameter ~15 nm) with polyacrylonitrile (PAN), which served as a precursor in the synthesis of ordered mesoporous carbons with large mesopores and high pore volume.⁶⁰ It was observed that the amount of the grafted polymer can be controlled by adjusting the time of polymerization. Later, our preliminary report noted that in cases of short polymerization times, when the mesopores of SBA-15 silica were not fully filled with PAN (and yet were inaccessible to gas molecules after the isolation of the silica/PAN composites), the grafted PAN had a relatively low polydispersity of 1.14–1.17.⁶¹ It was also possible to prepare FDU-1/PAN composite with accessible mesoporosity.⁶¹ Recently, the surface-initiated growth of polymer chains of low polydispersity (1.13–1.24) was achieved for ordered mesoporous material with pores of diameter ~8.5 nm.⁶² However, only in one case of well-controlled polymerization (in the presence of free initiator), the amount of the grafted polymer was commensurate with the pore volume of the silica support. In this case, the position of the capillary condensation step was

not shifted to any appreciable extent after the polymerization (despite a 20-fold decrease in adsorption capacity), revealing the lack of any significant pore diameter decrease and thus a very limited polymer growth in a part of the pore space. A recent study⁶³ showed that, by limiting the supply of the monomer, the grafting of polymer layer of thickness up to ~0.5 nm in the pores of SBA-15 silica can be accomplished without compromising the pore accessibility. The monomer/initiator ratio was varied to achieve different polymer layer thicknesses.

While the prior research afforded silica/polymer composites with accessible porosity and quite low polydispersity of the grafted polymer chains, little insight was gained into fundamental aspects of surface-initiated growth of polymer in narrow mesopores. In particular, an important question that was not addressed was to what extent the molecular weight of the polymer can be controlled in a way achievable for polymerizations in solution.³⁵ Moreover, questions whether the thickness of the polymer layer in narrow pores can be readily adjusted as in the best cases of polymerizations initiated from flat and convex surfaces^{19,37} and whether low polydispersities of grafted polymer (<1.1)^{64,65} can be achieved in polymerizations initiated from surfaces of narrow nanopores. To this end, it was recently suggested that the confinement effects increase polydispersities of grafted polymers even in pores as wide as 200 nm.⁶⁶ Herein, it is demonstrated that the surface-initiated ATRP (see Scheme 1) allows one to graft the surfaces of cylindrical and spherical mesopores (diameter 10–15 nm) of high-surface-area silicas with polymer chains of very low polydispersity (1.06–1.08), comparable to that attainable in well-controlled polymerizations in solution. Uniform polymer films of thickness tailorable up to 2.3 nm were successfully grown on the surfaces of the ordered mesoporous silicas, providing hybrid materials with accessible pores of uniform size and with specific surface areas of 70–350 m² g⁻¹.

Table 1. Conditions of Polymerization of Acrylonitrile Initiated from the Surface of FDU-1 and the Results of Characterization of the Grafted Polyacrylonitrile by GPC and TGA^a

sample	conditions	time (h)	wt % PAN	M_n (PS calibr)	PDI	DP	initiation efficiency (%)
FDU-1-PAN-1	0% Cu(II), 55 °C	18	33.3	15 700	1.12	53	33
FDU-1-PAN-2 ^b	0% Cu(II), 55 °C	92	38.5	18 200	1.32	61	36
FDU-1-PAN-3	10% Cu(II), 55 °C	92	37.6	17 000	1.34	57	37
FDU-1-PAN-4	10% Cu(II), 35 °C	18	17.7	9 600	1.06	32	23
FDU-1-PAN-5	20% Cu(II), 35 °C	18	14.8	8 200	1.07	28	22
FDU-1-PAN-6	20% Cu(II), 35 °C	44	21.1	9 100	1.06	31	30
FDU-1-PAN-7	20% Cu(II), 35 °C	68	27.8	10 900	1.07	37	37

^a Notation: wt % PAN = weight percent of PAN in silica–PAN composite estimated from TGA data for silica–BiB–TMS and silica–PAN composite and from the wt % Br for the former, assuming that the halogen exchange (exchange of Br by Cl at the polymer chain end) was complete; M_n = number-average molecular weight estimated by GPC calibrated using polystyrene (PS) standards; PDI = polydispersity index evaluated by GPC; DP = degree of polymerization evaluated under assumption that the molecular weight of PAN obtained using the PS calibration is overestimated by the factor of 5.59 (see Supporting Figure S1); initiation efficiency = estimated from DP, content of PAN (from TGA), and amount of surface-bonded initiator. ^b Sample was used elsewhere⁶⁰ to obtain an ordered mesoporous carbon.

Materials and Methods

Materials. SBA-15 silica with cylindrical pores of diameter ~10 nm and FDU-1 silica with spherical pores of diameter ~15 nm were synthesized as described elsewhere.^{59,60,67} The characterization of the FDU-1 sample was reported earlier.⁶⁰ The surfaces of the silicas were reacted with 3-(chlorodimethylsilyl)propyl 2-bromoisobutyrate (ATRP initiator) and subsequently with chlorotrimethylsilane.^{60,68} (2-Bromoisobutyryloxy)propyldimethylsilyl groups are denoted BiB. The reaction with chlorotrimethylsilane was performed to introduce small trimethylsilyl (TMS) groups between the larger BiB groups, thus hindering the possible adsorption of copper complexes on the bare surface of the silica support. For the surface-initiated polymerization of acrylonitrile (AN), the molar ratio of reactants was as follows: BiB:AN:CuCl:CuCl₂:bpy = 1:300:1: x :2 + 2*x*, where x = 0 (0%), 0.1 (10%), or 0.2 (20%) and bpy is 2,2'-bipyridine. The polymerization was carried out in DMF (DMF/AN volume ratio of 1.74:1) at 35 or 55 °C. For x = 0 and temperature of 55 °C, these conditions are analogous to those used in our earlier work.⁶⁰ For the surface-initiated polymerization of 2-(dimethylamino)ethyl methacrylate (DMAEMA), the reactant molar ratios were similar (BiB:DMAEMA:CuCl:CuCl₂:bpy = 1:300:1:0.1:2.2); acetone was used as a solvent, and the temperature was 35 °C. The polymerization time was between 18 and 162 h for PAN and between 2 and 25 h for PDMAEMA. For PS, the conditions are provided in the Supporting Information. The polymer/silica composites were isolated by filtration, washed with DMF (for PAN) or acetone (for PDMAEMA and PS) and methanol, and dried in a vacuum oven.

Measurements. Nitrogen adsorption isotherms were measured on Micromeritics ASAP 2010 and ASAP 2020 volumetric adsorption analyzers. The specific surface area was determined using the BET method.²⁰ The total pore volume was calculated from the amount adsorbed at a relative pressure of 0.99.²⁰ The pore size distribution was calculated using the KJS method for cylindrical mesopores.⁶⁹ The weight change patterns were recorded under air using a TA Instruments TGA 2950 thermogravimetric analyzer. Elemental analysis for carbon and bromine was carried out by Midwest Microlab, LLC (Indianapolis, IN). Molecular weight distributions of grafted PAN and PS were determined via gel permeation chromatography (GPC) using DMF (for PAN) or THF (for PS) as an eluent and polystyrenes as standards. The polystyrene calibration results in the molecular weight overestimation by the factor of ~5.59 for PAN of molecular weight in the range observed for our grafted polymers (see Figure S1 of the Supporting Information). Therefore, molecular weights of PAN determined by GPC were divided by 5.59 in calculations of the actual molecular weight. For GPC analysis, the polymer was isolated through the dissolution of the silica support using 48% HF water solution mixed with DMF (for PAN) and THF (for PS) in the volume ratio of one to one.

Results and Discussion

The polymerization of acrylonitrile (AN) initiated from the surfaces of ordered mesoporous silicas (OMSs) with spherical

and cylindrical pore geometries was selected for our initial study, which was in part due to our long-standing interest in this polymer as a precursor for nanostructured carbon synthesis.^{57,60,65,70–72} One of the silica supports used was FDU-1 silica^{60,67,73} with approximately spherical mesopores of diameter 14.4 nm, as estimated using the KJS method for calculation of pore size distributions (PSDs)⁶⁹ (a more accurate estimate of the pore diameter performed on the basis of the unit-cell parameter, mesopore volume, and micropore volume⁷⁴ yields 17.5 nm). The ATRP initiation sites were introduced on the surface of the silica support through a reaction with 3-(chlorodimethylsilyl)propyl 2-bromoisobutyrate.⁶⁰ The chlorosilane moiety reacted with the silanol groups (Si–OH) on the silica surface to form Si–O–Si linkages. The attached 3-(2-bromoisobutyryloxy)propyldimethylsilyl groups (BiB) exhibited a surface coverage of 1.26 $\mu\text{mol m}^{-2}$ (0.76 group nm^{-2}), as calculated from the bromine content determined by elemental analysis and the silica content determined using thermogravimetry.

The controlled growth of polymers through ATRP requires the presence of sufficient amount of deactivator (oxidized form of the catalytic complex; Cu(II) complex in the considered case) in the reaction mixture in order to convert growing polymer chains with radical ends to dormant species and thus limit the concentration of the radicals to reduce their coupling and to allow for their controlled growth.³⁵ The concentration of Cu(II) species builds up as the polymerization proceeds, but it is beneficial to introduce copper(II) species before the beginning of the polymerization. Controlled polymerizations also require a fast initiation of the growth of the polymer chains with respect to their propagation. To promote that, the halogen exchange method was used; that is, a more reactive brominated initiator was used in combination with copper(I) chloride and copper(II) chloride as components of the ATRP catalyst.³⁵ This is known to lead to an exchange of the bromide by chloride at the end of the growing polymer chain, and it slows down the propagation relative to the initiation.⁷⁵ On the basis of these considerations and our earlier work,^{56,61} the PAN grafting on the surface of FDU-1 silica was carried out with the following molar ratios of reagents: BiB:AN:CuCl:CuCl₂:bpy = 1:300:1: x :2 + 2*x*, where x = 0 (0%), 0.1 (10%), and 0.2 (20%). The catalyst was a complex of copper(I) with 2,2'-bipyridine (bpy). The solvent was *N,N*-dimethylformamide (DMF) (DMF/AN volume ratio was 1.74 to 1), and the temperature was either 55 or 35 °C (for conditions used in cases of particular samples; see Table 1).

As seen in Figure 1, the amount of the introduced PAN strongly depended on whether CuCl₂ was used as a reagent in order to facilitate the deactivation during initial stages of the polymerization. The amount of PAN introduced after 92 h of polymerization (0% or 10% CuCl₂) was close to the limit of the complete filling of the mesopores (as estimated from the

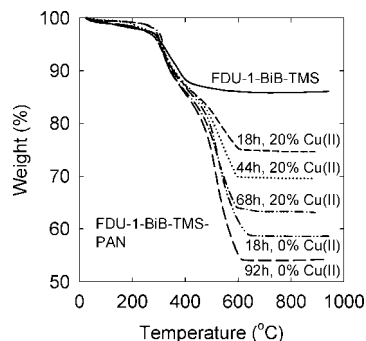


Figure 1. Weight change patterns recorded under air for FDU-1 silica with surface-bonded 2-bromoisobutyrate groups and trimethylsilyl groups (–BiB–TMS), before and after acrylonitrile polymerization for different periods of time (in some cases with addition of CuCl_2).

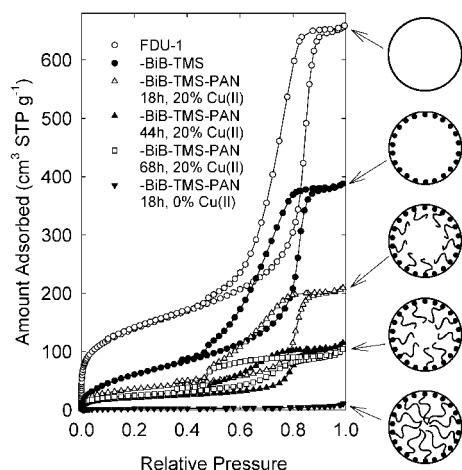


Figure 2. Nitrogen adsorption isotherms for FDU-1 silica before and after bonding of 2-bromoisobutyrate groups and trimethylsilyl groups (–BiB–TMS) and after acrylonitrile polymerization for different periods of time. The schemes on the right illustrate the stage of the synthesis corresponding to the particular adsorption isotherm.

Table 2. Structural Properties of the FDU-1 Samples Determined from Nitrogen Adsorption Data

silica	BET specific surface area ($\text{m}^2 \text{g}^{-1}$)	total pore volume ($\text{cm}^3 \text{g}^{-1}$)	pore diameter (nm)
FDU-1	500 ^a	1.01 ^a	14.4 ^{a,b}
FDU-1-BiB	260 ^a	0.63 ^a	13.3 ^{a,b}
FDU-1-BiB-TMS	240 ^a	0.60 ^a	13.0 ^{a,b}
FDU-1-PAN-4	119	0.29	11.6 ^b
FDU-1-PAN-5	132	0.32	11.8 ^b
FDU-1-PAN-6	75	0.18	10.9 ^b
FDU-1-PAN-7	91	0.16	8.3 ^b

^a Data taken from ref 60. ^b Actual pore diameter is likely to be ~ 3 nm larger than the values provided.

pore volume of the silica and the weight loss of the silica/polymer composite under an assumption that the density of the organic moiety in the pores is $\sim 1.0 \text{ g cm}^{-3}$. The pores of FDU-1 appeared to be also nearly fully filled after 18 h of polymerization, when CuCl_2 was not added. On the other hand, the addition of CuCl_2 slowed down the polymerization process. In the case of addition of 20% CuCl_2 (with respect to the amount of CuCl), the amount of PAN gradually increased with time, as seen from TGA (see Figure 1). The PAN grafting resulted in a gradual decrease in the adsorption capacity (see Figure 2 and total pore volume data in Table 2). The position of the peak on the pore size distribution (PSD) systematically shifted to lower pore diameter values as the PAN content increased, and no major broadening of PSD was observed (Figure 3). To our

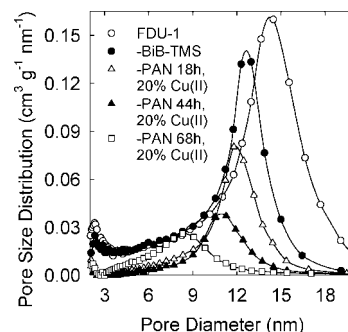


Figure 3. Pore size distributions for FDU-1 silica before and after bonding of 2-bromoisobutyrate groups and trimethylsilyl groups (–BiB–TMS) and after acrylonitrile polymerization for different periods of time.

knowledge, this is the first example of a systematic control of the pore diameter of OMS through the surface-initiated polymerization. Others achieved a limited adjustment of pore diameter of OMS through the variation of the surface density of the initiator or the use of limited supply of monomer.⁶³ In our case, the growth of the polymer was gradual, and different polymer film thicknesses and polymer loadings can be obtained using the same composition of the reaction mixture simply by stopping the polymerization after an appropriate period of time.

The shape of adsorption–desorption hysteresis loop did not change until the loading of organic groups in mesopores reached $\sim 0.4 \text{ g}$ per gram of silica, indicating that the growth of the polymer did not obstruct the connectivity between the spherical mesopores of FDU-1, unless the polymer loading was very high. These results provide strong evidence that the formation of the PAN layer was uniform throughout the surface of the silica support. In the considered case, the thickness of the PAN layer was 0.6–2.3 nm, as calculated from the decrease in the pore radius after the polymerization. The BET specific surface area of the obtained well-defined FDU-1/PAN composites was about $100 \text{ m}^2 \text{g}^{-1}$, while the total pore volume was on the order of $0.25 \text{ cm}^3 \text{g}^{-1}$. It can be concluded that the formation of a very thin, uniform PAN film of controlled thickness was achieved on high-surface-area silica supports, thus generating silica/polymer composites with accessible porosity and appreciable surface area and pore volume. As preliminarily reported earlier, in the case of one sample of FDU-1, we were able to graft a thin film of PAN without pore blockage, when CuCl_2 was not added as a deactivator.⁶¹ However, the film appeared to be less uniform, as inferred from the comparison of PSDs. More recently, the feasibility of ATRP of methyl methacrylate (MMA) and glycidyl methacrylate (GMA) initiated from surface of SBA-15 silica was studied, and uniform polymer layers of thickness up to $\sim 0.5 \text{ nm}$ were grafted.⁶³ The thickness of these relatively very thin films was controlled by changing the initiator/monomer ratio (which was in all cases very low, that is, from 5:1 to 25:1) rather than the polymerization time or other conditions.

As seen in Figure 4 and in Table 1, the grafted PAN had low polydispersity. After 18 h, the polydispersity was 1.12 when Cu(II) halide was not added. The polydispersity was even lower (1.06–1.07) when Cu(II) halide was added. Such a low polydispersity index is comparable to the lowest values attainable for ATRP in solutions³⁵ or surface-initiated ATRP.^{64,65} It should be noted that the use of PS standards for PAN is expected to provide good estimates of polydispersity. It was shown that apparent polydispersity of polymer 1 (calibrated using standards of polymer 2) is equal to the actual polydispersity taken to the power of $(a_1 + 1)/(a_2 + 1)$, where a_1 and a_2 are the Mark–Houwink constants for the considered polymer 1 and for the polymer 2 used for calibration.⁷⁶ Using $a_1 = 0.750$ (for PAN) and $a_2 = 0.603$ (for PS),⁷⁷ one finds that actual

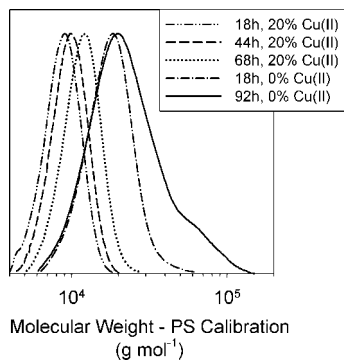


Figure 4. Gel permeation chromatography traces for PAN isolated from FDU-1/PAN composites.

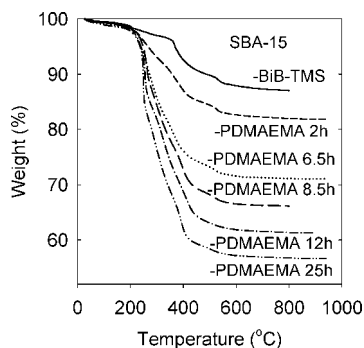


Figure 5. Weight change patterns recorded under air for the SBA-15 silica with surface-bonded $-\text{Si}(\text{CH}_3)_2[(\text{CH}_2)_3-\text{O}-\text{CO}-\text{C}(\text{CH}_3)_2\text{Br}]$ groups and $-\text{Si}(\text{CH}_3)_3$ groups (denoted -BiB-TMS) before and after the polymerization of 2-(dimethylamino)ethyl methacrylate for different periods of time ranging from 2 to 25 h.

polydispersity for PAN is equal to (apparent) polydispersity for PAN with PS calibration taken to the power of 1.192. For instance, the polydispersity of 1.06 corresponds to the actual polydispersity of 1.07. So the calibration using standards of a different polymer does not affect the discussed polydispersities to any appreciable extent.

Our lowest polydispersity values of 1.06–1.07 are appreciably lower than those reported by Save et al.^{55,62} (1.13–1.41 in the presence of free initiator and 1.23–2.59 in the absence of free initiator) and in our earlier work⁶¹ (1.14–1.58) where Cu(II) halide was not employed. The increase in the molecular weight of PAN was correlated with the content of the polymer in silica/PAN composites (determined from TGA). For long polymerization times (about 4 days), in which case the pores were essentially completely filled with the polymer, the polydispersity increased to ~ 1.3 , and a “tailing” toward higher molecular weights developed on the molecular weight distribution (see Figure 4). The origin of the “tailing” is not fully clear. The “tailing” may represent a population of polymer chains grown on the external surface of particles of FDU-1. While the growth of polymer chains inside the pores was hindered because of the scarcity of available space, the chains growing on the external surface had no such restriction. Alternatively, at the stage where the pores were nearly completely filled with polymer, the diffusion of the deactivator (Cu(II) complex) may have been restricted and some of the growing radical chains were not converted to the dormant form, but rather they underwent uncontrolled growth, consuming the residual amounts of monomer remaining in the pores, or coupled, forming dead chains with doubled molecular weight.

The degree of polymerization (DP) was estimated to range from 28 to 61, depending on the polymerization conditions. For the same polymerization conditions, DP increased with time.

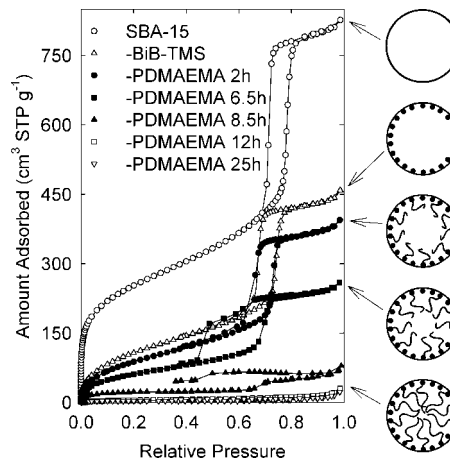


Figure 6. Nitrogen adsorption isotherms for SBA-15 silica and the SBA-15 with surface-bonded $-\text{Si}(\text{CH}_3)_2[(\text{CH}_2)_3-\text{O}-\text{CO}-\text{C}(\text{CH}_3)_2\text{Br}]$ groups and $-\text{Si}(\text{CH}_3)_3$ groups (denoted -BiB-TMS), before and after the polymerization of 2-(dimethylamino)ethyl methacrylate for different periods of time from 2 to 25 h. The schemes on the right illustrate the stage of the synthesis corresponding to the particular adsorption isotherm.

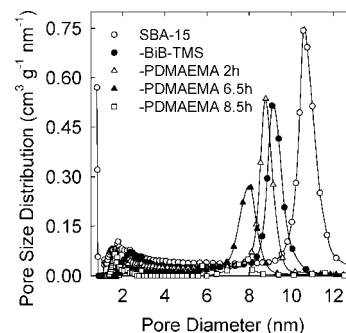


Figure 7. Pore size distributions for SBA-15 silica and the SBA-15 with surface-bonded $-\text{Si}(\text{CH}_3)_2[(\text{CH}_2)_3-\text{O}-\text{CO}-\text{C}(\text{CH}_3)_2\text{Br}]$ groups and $-\text{Si}(\text{CH}_3)_3$ groups (denoted -BiB-TMS), before and after the polymerization of 2-(dimethylamino)ethyl methacrylate for different periods of time from 2 to 25 h.

DP decreased with the increase in the amount of Cu(II) added, when the time of the polymerization was kept constant. The efficiency of initiation, that is, the ratio of the number of grafted polymer chains to the number of initiation sites, was 22–37%, so the initiation was not quantitative. In exceptional cases of the surface-initiated polymerization, the initiation efficiency was reported to be up to 60–80% on convex surfaces,^{65,78} but typically observed initiation efficiencies on flat or convex surfaces^{15,19,44,79} were lower or at best comparable to our results for concave surfaces. Taking into account the concave surface geometry, which is likely to sterically restrict the polymer growth when compared to flat or convex surfaces, our initiation efficiencies were high. The polymer grafting density was 0.17–0.28 chains/nm². Earlier studies of polymerization initiated from the flat surfaces^{28,80–82} and convex surfaces^{83–85} of nanoparticles provided graft density estimates ranging from very low values up to 0.6–1.0 chains/nm², although grafting densities of ~ 0.1 –0.4 chains/nm² were very common.^{45,86–88} A review by Tsujii et al.¹⁹ mentioned that the grafting density of 0.6 chains/nm² was achieved for the silica monolith with pore diameter of ~ 50 nm, which is much larger than the diameter of the pores considered herein. Save et al. reported the grafting density of 0.05 chains/nm² and the initiation efficiency of 5% in the case of the synthesis of polymer-grafted OMS with accessible pores.⁶² Given that in our case the polymerization was initiated from concave surfaces of appreciable degree of

curvature, and the polymer growth was restricted by the limited pore dimensions (see schemes in Figure 2), the attained grafting density appears to be appreciable.

Very low polydispersities of the polymer graft and the initiation efficiencies of 17–35% were also observed for the PAN growth in cylindrical mesopores of SBA-15 silica (see Table S1 and Figure S2 of the Supporting Information). Narrow PSDs and the decrease in the pore diameter consistent with the amount of introduced PAN were observed for 10–22 wt % loadings (see Figures S3 and S4 of the Supporting Information). However, in the case of both samples with 22% loading, PSDs were noticeably broader than the PSD of the SBA-15 support, and the adsorption–desorption hysteresis loops on adsorption isotherms were quite broad, thus indicating the development of constrictions in the porous structure as a result of the polymer grafting. The constrictions may be related to the roughness of the polymer-covered surface or to the bridging of the inner pore space by single PAN chains or bundles of chains. The BET specific surface area of these well-defined SBA-15/PAN composites was about $300 \text{ m}^2 \text{ g}^{-1}$, while the total pore volume was about $0.4 \text{ cm}^3 \text{ g}^{-1}$. For 32 wt % PAN loading, the primary mesopores still appeared to be accessible, but a narrow PSD peak was no longer observed, probably due to the roughness of PAN film and/or bridging of PAN chains across the mesopores.

The total pore volume of SBA-15 was higher than that of FDU-1, so one would expect that SBA-15 could accommodate a higher PAN loading without the pore blocking than FDU-1 could. Since it was not observed, one can conclude that the larger pore diameter and better pore connectivity (larger number of entrances per pore) allow one to introduce a higher loading of PAN in pores of FDU-1 without broadening of PSD. Our subsequent study⁸⁹ confirmed that larger pore diameter of cylindrical pores ($\sim 15 \text{ nm}$) indeed allows one to introduce higher polymer loadings without the pore blocking. Another interesting aspect was that the initiation efficiencies were below 100%, despite the fact that the coverage of BiB groups on the surfaces of SBA-15 and FDU-1 was moderate (0.30 and 0.76 groups/nm², respectively). Perhaps some of the 2-bromoisobutyrate groups were located in the micropores of FDU-1 and SBA-15 silicas and thus were not accessible to initiate polymerization. However, this is not likely to account for the observed initiation from less than half of the sites. Perhaps the concave shape of the surface (see schemes in Figure 2) contributed to the reduced initiation efficiency.

The results presented above indicate that one can graft uniform thin layers of PAN on surfaces of high-surface-area nanoporous silicas using the surface-initiated ATRP. To confirm the generality of this finding, poly[2-(dimethylamino)ethyl methacrylate] (PDMAEMA) was grafted from surfaces of SBA-15 and FDU-1 silicas. PDMAEMA is a pH-responsive and temperature-responsive polymer with lower critical solution temperature of $\sim 44^\circ\text{C}$.^{90–93} As shown in Figure 5, TGA provided evidence for the systematic increase in the amount of PDMAEMA with the polymerization time. The content of organic groups attained after 25 h of polymerization is likely to correspond to a nearly complete filling of the mesopores of the SBA-15 silica with the surface-initiated polymer graft. Gas adsorption (Figure 6) showed that the SBA-15/PDMAEMA composites with 7 and 19 wt % of polymer exhibited accessible pores of volume $0.40\text{--}0.61 \text{ cm}^3 \text{ g}^{-1}$, and specific surface areas of $240\text{--}350 \text{ m}^2 \text{ g}^{-1}$ (see Table S3 of the Supporting Information). No appreciable broadening of the pore size distribution (PSD) was observed (see Figure 7) as a result of the grafting of the polymer. For longer polymerization times, which led to the PDMAEMA content of 24–35%, the pores became partially or fully inaccessible. It should be noted that the analysis of PDMAEMA by GPC was unsuccessful, presumably due to the

protonation of the amino groups during the HF etching. The grafting of PDMAEMA in spherical pores of FDU-1 was also studied and the FDU-1/PDMAEMA composite with 20 wt % of the polymer was readily obtained with accessible porosity and narrow PSD (see Figures S5 and S6 and Table S3 of the Supporting Information). The FDU-1/PDMAEMA composite with 38 wt % of the polymer was also prepared but had inaccessible pores.

To additionally confirm the ability to graft highly monodisperse polymer chains in nanopores using ATRP, the surface-initiated growth of polystyrene was studied, so that the molecular weight of detached PS chains could be assessed using GPC without recalculation. TGA, gas adsorption, and GPC data for selected samples are provided as Supporting Information (Figures S7–S9 and Table S4). As in the cases of PAN and PDMAEMA, the content of the grafted polymer was controlled by the polymerization time, and it was possible to obtain materials with accessible pores and narrow PSD. For short polymerization times of 4.5 and 8 h (no halogen exchange), the molecular weights were 1670 and 2270 g mol^{-1} (degree of polymerization 16 and 22), and the polydispersity indexes were 1.08 and 1.20, respectively. The initiation efficiency was estimated to be 9% and 12%, being somewhat lower than that attained for PAN, but of the same order of magnitude. These results show that short PS chains of low polydispersity can be grafted from ordered mesoporous silica surface, which is consistent with our results on PAN grafting. On the other hand, the polydispersity of PS appeared to increase significantly with time of polymerization (or loading of PS). The samples obtained after 8 h with halogen exchange and after 24 h without halogen exchange gave very broad molecular weight distributions with polydispersity indexes of 2.09 and 2.92. These results may be related to high glass transition temperature of PS and vitrification of the reaction mixture inside the pores. In order to ensure catalyst homogeneity in ATRP of styrene,³⁴ $[\text{Cu}(\text{I})\text{dNbpy}_2]^+$ and $[\text{Br}-\text{Cu}(\text{II})\text{dNbpy}_2]^+$ complexes (ATRP catalyst and deactivator) were used. The 4-nonyl substituents on 2,2'-bipyridine increase the size of the catalyst complex and may decrease its effective diffusion in the pores of SBA-15, especially after their size has already been reduced by the PS graft and viscosity strongly increased by approaching the glass transition.

Conclusions

Atom-transfer radical polymerization (ATRP) allows one to graft highly monodisperse polymer chains (PDI as low as 1.06–1.08) from surfaces of high-surface-area silicas with nanopores of diameter $\sim 10\text{--}15 \text{ nm}$. The grafted polymer forms a uniform layer of thickness tailorable in the range from several tenths of a nanometer to at least 2 nm. The control in the adjustment of the thickness of the polymer film is improved, the pore blocking is mitigated, and the polydispersity is minimized when Cu(II) halide is added as a deactivator to the reaction mixture. If the amount of the surface-grafted polymer does not approach the level needed to fill the pores completely, the pores in the polymer–silica hybrids prepared under optimized conditions are accessible in many cases, and pore size distributions are similarly narrow as those of the corresponding silica supports. The specific surface areas attained for the silica/polymer composites prepared using the surface-initiated ATRP ranged from 75 to $350 \text{ m}^2 \text{ g}^{-1}$. The approach described herein for the synthesis of silica/polymer composites promises to be applicable to a wide variety of polymers that can be polymerized in a controlled way via ATRP.

Acknowledgment. Pasquale Fulvio (Kent State University) is acknowledged for the synthesis of SBA-15 silica. The support from NSF Grant DMR-0304508 is gratefully acknowledged. T.K. and K.M. also acknowledge support from NSF Grant DMR-0549353.

Supporting Information Available: Four tables and nine figures showing experimental GPC, TGA, gas adsorption, and pore size distribution data. This material is available free of charge via the Internet at <http://pubs.acs.org>.

References and Notes

- Wu, C. G.; Bein, T. *Science* **1994**, *264*, 1757–1759.
- Wu, C.-G.; Bein, T. *Science* **1994**, *266*, 1013–1015.
- Nguyen, T.-Q.; Wu, J.; Doan, V.; Schwartz, B. J.; Tolbert, S. H. *Science* **2000**, *288*, 652–656.
- Lu, Y.; Yang, Y.; Sellinger, A.; Lu, M.; Huang, J.; Fan, H.; Haddad, R.; Lopez, G.; Burns, A. R.; Sasaki, D. Y.; Shelnutt, J.; Brinker, C. J. *Nature (London)* **2001**, *410*, 913–917.
- Johnson, S. A.; Ollivier, P. J.; Mallouk, T. E. *Science* **1999**, *283*, 963–965.
- Kageyama, K.; Tamazawa, J.-I.; Aida, T. *Science* **1999**, *285*, 2113–2115.
- Sozzani, P.; Bracco, S.; Comotti, A.; Simonutti, R.; Valsesia, P.; Sakamoto, Y.; Terasaki, O. *Nat. Mater.* **2006**, *5*, 545–551.
- Huber, D. L.; Manginell, R. P.; Samara, M. A.; Kim, B. I.; Bunker, B. C. *Science* **2003**, *301*, 352–354.
- Choi, M.; Kleitz, F.; Liu, D.; Lee, H. Y.; Ahn, W.-S.; Ryoo, R. *J. Am. Chem. Soc.* **2005**, *127*, 1924–1932.
- Prucker, O.; Ruhe, J. *Macromolecules* **1998**, *31*, 592–601.
- Huang, X.; Wirth, M. J. *Anal. Chem.* **1997**, *69*, 4577–4580.
- Meyer, U.; Svec, F.; Frechet, J. M. J.; Hawker, C. J.; Irgum, K. *Macromolecules* **2000**, *33*, 7769–7775.
- Zhao, B.; Brittain, W. J. *Prog. Polym. Sci.* **2000**, *25*, 677–710.
- Pyun, J.; Kowalewski, T.; Matyjaszewski, K. *Macromol. Rapid Commun.* **2003**, *24*, 1043–1059.
- Edmondson, S.; Osborne, V. L.; Huck, W. T. S. *Chem. Soc. Rev.* **2004**, *33*, 14–22.
- Boyes, S. G.; Granville, A. M.; Baum, M.; Akgun, B.; Mirois, B. K.; Brittain, W. J. *Surf. Sci.* **2004**, *570*, 1–12.
- Jennings, G. K.; Brantley, E. L. *Adv. Mater.* **2004**, *16*, 1983–1994.
- Ruhe, J.; Ballauff, M.; Biesalski, M.; Dziezok, P.; Grohn, F.; Johannsmann, D.; Houben, N.; Hugenberg, N.; Konradi, R.; Minko, S.; Motornov, M.; Netz, R. R.; Schmidt, M.; Seidel, C.; Stamm, M.; Stephan, T.; Usov, D.; Zhang, H. N. *Adv. Polym. Sci.* **2004**, *165*, 79–150.
- Tsujii, Y.; Ohno, K.; Yamamoto, S.; Goto, A.; Fukuda, T. *Adv. Polym. Sci.* **2006**, *197*, 1–45.
- Sing, K. S. W.; Everett, D. H.; Haul, R. A. W.; Moscou, L.; Pierotti, R. A.; Rouquerol, J.; Siemieniowska, T. *Pure Appl. Chem.* **1985**, *57*, 603–619.
- Cho, M. S.; Choi, H. J.; Kim, K. Y.; Ahn, W. S. *Macromol. Rapid Commun.* **2002**, *23*, 713–716.
- Sasidharan, M.; Mal, N. K.; Bhaumik, A. J. *Mater. Chem.* **2007**, *17*, 278–283.
- Reynhardt, J. P. K.; Yang, Y.; Sayari, A.; Alper, H. *Chem. Mater.* **2004**, *16*, 4095–4102.
- Acosta, E. J.; Carr, C. S.; Simanek, E. E.; Shantz, D. F. *Adv. Mater.* **2004**, *16*, 985–989.
- Ejaz, M.; Yamamoto, S.; Ohno, K.; Tsujii, Y.; Fukuda, T. *Macromolecules* **1998**, *31*, 5934–5936.
- Jordan, R.; Ulman, A. J. *Am. Chem. Soc.* **1998**, *120*, 243–247.
- Huang, X.; Wirth, M. J. *Macromolecules* **1999**, *32*, 1694–1696.
- Hussemann, M.; Malmstrom, E. E.; McNamara, M.; Mate, M.; Mecerreyes, D.; Benoit, D. G.; Hedrick, J. L.; Mansky, P.; Huang, E.; Russell, T. P.; Hawker, C. J. *Macromolecules* **1999**, *32*, 1424–1431.
- Matyjaszewski, K.; Miller, P. J.; Shukla, N.; Immaraporn, B.; Gelman, A.; Luokala, B. B.; Siclovian, T. M.; Kickelbick, G.; Vallant, T.; Hoffmann, H.; Pakula, T. *Macromolecules* **1999**, *32*, 8716–8724.
- von Werne, T.; Patten, T. E. *J. Am. Chem. Soc.* **1999**, *121*, 7409–7410.
- Zhao, B.; Brittain, W. J. *J. Am. Chem. Soc.* **1999**, *121*, 3557–3558.
- Wang, J.-S.; Matyjaszewski, K. *J. Am. Chem. Soc.* **1995**, *117*, 5614–5615.
- Kato, M.; Kamigaito, M.; Sawamoto, M.; Higashimura, T. *Macromolecules* **1995**, *28*, 1721–1723.
- Patten, T. E.; Xia, J. H.; Abernathy, T.; Matyjaszewski, K. *Science* **1996**, *272*, 866–868.
- Matyjaszewski, K.; Xia, J. *Chem. Rev.* **2001**, *101*, 2921–2990.
- Huang, X.; Doneski, L. J.; Wirth, M. J. *Anal. Chem.* **1998**, *70*, 4023–4029.
- Ejaz, M.; Ohno, K.; Tsujii, Y.; Fukuda, T. *Macromolecules* **2000**, *33*, 2870–2874.
- Yamamoto, S.; Ejaz, M.; Tsujii, Y.; Matsumoto, M.; Fukuda, T. *Macromolecules* **2000**, *33*, 5602–5607.
- Ejaz, M.; Tsujii, Y.; Fukuda, T. *Polymer* **2001**, *42*, 6811–6815.
- Zhao, B.; Brittain, W. J. *Macromolecules* **2000**, *33*, 8813–8820.
- Yu, W. H.; Kang, E. T.; Neoh, K. G.; Zhu, S. P. *J. Phys. Chem. B* **2003**, *107*, 10198–10205.
- Jones, D. M.; Huck, W. T. S. *Adv. Mater.* **2001**, *13*, 1256–1259.
- Jones, D. M.; Smith, J. R.; Huck, W. T. S.; Alexander, C. *Adv. Mater.* **2002**, *14*, 1130–1134.
- Jones, D. M.; Brown, A. A.; Huck, W. T. S. *Langmuir* **2002**, *18*, 1265–1269.
- Tsujii, Y.; Ejaz, M.; Sato, K.; Goto, A.; Fukuda, T. *Macromolecules* **2001**, *34*, 8872–8878.
- Baum, M.; Brittain, W. J. *Macromolecules* **2002**, *35*, 610–615.
- Zhao, B. *Polymer* **2003**, *44*, 4079–4083.
- Habaue, S.; Ikeshima, O.; Ajiro, H.; Okamoto, Y. *Polym. J.* **2001**, *33*, 902–905.
- Fu, Q.; Rao, G. V. R.; Basame, S. B.; Keller, D. J.; Artyushkova, K.; Fulghum, J. E.; Lopez, G. P. *J. Am. Chem. Soc.* **2004**, *126*, 8904–8905.
- Schepelina, O.; Zharov, I. *Langmuir* **2006**, *22*, 10523–10527.
- Liu, B.; Jin, Z.; Qu, X.; Yang, Z. *Macromol. Rapid Commun.* **2007**, *28*, 322–328.
- Fu, Q.; Rao, G. V. R.; Ista, L. K.; Wu, Y.; rzejewski, B. P.; Sklar, L. A.; Ward, T. L.; Lopez, G. P. *Adv. Mater.* **2003**, *15*, 1262–1266.
- Lenarda, M.; Chessa, G.; Moretti, E.; Polizzi, S.; Storaro, L.; Talon, A. *J. Mater. Sci.* **2006**, *41*, 6305–6312.
- Chung, P.-W.; Kumar, R.; Pruski, M.; Lin, V. S.-Y. *Adv. Funct. Mater.* **2008**, *18*, 1–9.
- Audouin, F.; Blas, H.; Pasetto, P.; Beaunier, P.; Boissiere, C.; Sanchez, C.; Save, M.; Charleux, B. *Macromol. Rapid Commun.* **2008**, *29*, 914–921.
- Kruk, M.; Dufour, B.; Celer, E. B.; McCullough, L.; Kowalewski, T.; Jaroniec, M.; Matyjaszewski, K. *Polym. Prepr.* **2005**, *46*, 156–157.
- Kruk, M.; Dufour, B.; Celer, E. B.; McCullough, L.; Jaroniec, M.; Matyjaszewski, K.; Kowalewski, T. *Polym. Prepr.* **2005**, *46*, 173–174.
- Zhou, Z.; Zhu, S.; Zhang, D. J. *Mater. Chem.* **2007**, *17*, 2428–2433.
- Zhao, D.; Feng, J.; Huo, Q.; Melosh, N.; Frederickson, G. H.; Chmelka, B. F.; Stucky, G. D. *Science* **1998**, *279*, 548–552.
- Kruk, M.; Dufour, B.; Celer, E. B.; Kowalewski, T.; Jaroniec, M.; Matyjaszewski, K. *J. Phys. Chem. B* **2005**, *109*, 9216–9225.
- Kruk, M.; Dufour, B.; Celer, E. B.; Kowalewski, T.; Jaroniec, M.; Matyjaszewski, K. *Polym. Mater. Sci. Eng.* **2007**, *97*, 274–275.
- Save, M.; Granvorka, G.; Bernard, J.; Charleux, B.; Boissiere, C.; Grosso, D.; Sanchez, C. *Macromol. Rapid Commun.* **2006**, *27*, 393–398.
- Moreno, J.; Sherrington, D. C. *Chem. Mater.* **2008**, *20*, 4468–4474.
- Boyes, S. G.; Brittain, W. J.; Weng, X.; Cheng, S. Z. D. *Macromolecules* **2002**, *35*, 4960–4967.
- Tang, C.; Bombalski, L.; Kruk, M.; Jaroniec, M.; Matyjaszewski, K.; Kowalewski, T. *Adv. Mater.* **2008**, *20*, 1516–1522.
- Gorman, C. B.; Petrie, R. J.; Genzer, J. *Macromolecules* **2008**, *41*, 4856–4865.
- Yu, C.; Yu, Y.; Zhao, D. *Chem. Commun.* **2000**, 575–576.
- Savin, D. A.; Pyun, J.; Patterson, G. D.; Kowalewski, T.; Matyjaszewski, K. *J. Polym. Sci., Part B: Polym. Phys.* **2002**, *40*, 2667–2676.
- Kruk, M.; Jaroniec, M.; Sayari, A. *Langmuir* **1997**, *13*, 6267–6273.
- Kowalewski, T.; Tsarevsky, N. V.; Matyjaszewski, K. *J. Am. Chem. Soc.* **2002**, *124*, 10632–10633.
- Tang, C.; Qi, K.; Wooley, K. L.; Matyjaszewski, K.; Kowalewski, T. *Angew. Chem., Int. Ed.* **2004**, *43*, 2783–2787.
- Tang, C. B.; Tracz, A.; Kruk, M.; Zhang, R.; Smilgies, D. M.; Matyjaszewski, K.; Kowalewski, T. *J. Am. Chem. Soc.* **2005**, *127*, 6918–6919.
- Matos, J. R.; Kruk, M.; Mercuri, L. P.; Jaroniec, M.; Zhao, L.; Kamiyama, T.; Terasaki, O.; Pinnavaia, T. J.; Liu, Y. *J. Am. Chem. Soc.* **2003**, *125*, 821–829.
- Ravikovitch, P. I.; Neimark, A. V. *Langmuir* **2002**, *18*, 1550–1560.
- Matyjaszewski, K.; Shipp, D. A.; Wang, J.-L.; Grimaud, T.; Patten, T. E. *Macromolecules* **1998**, *31*, 6836–6840.
- Netopilik, M.; Kratochvil, P. *Polymer* **2003**, *44*, 3431–3436.
- Morariu, S.; Bercea, M.; Ioan, C.; Ioan, S.; Simionescu, B. C. *Eur. Polym. J.* **1999**, *35*, 377–383.
- El Harrak, A.; Carrot, G.; Oberdisse, J.; Eychenne-Baron, C.; Boue, F. *Macromolecules* **2004**, *37*, 6376–6384.
- Kizhakkedathu, J. N.; Brooks, D. E. *Macromolecules* **2003**, *36*, 591–598.
- Devaux, C.; Cousin, F.; Beyou, E.; Chapel, J. P. *Macromolecules* **2005**, *38*, 4296–4300.
- Yamamoto, S.; Ejaz, M.; Tsujii, Y.; Fukuda, T. *Macromolecules* **2000**, *33*, 5608–5612.
- Zhao, B. *Langmuir* **2004**, *20*, 11748–11755.
- Li, D. J.; Sheng, X.; Zhao, B. *J. Am. Chem. Soc.* **2005**, *127*, 6248–6256.

- (84) Marutani, E.; Yamamoto, S.; Ninjbadgar, T.; Tsujii, Y.; Fukuda, T.; Takano, M. *Polymer* **2004**, *45*, 2231–2235.
- (85) Ohno, K.; Morinaga, T.; Koh, K.; Tsujii, Y.; Fukuda, T. *Macromolecules* **2005**, *38*, 2137–2142.
- (86) Matsuno, R.; Yamamoto, K.; Otsuka, H.; Takahara, A. *Macromolecules* **2004**, *37*, 2203–2209.
- (87) Feng, W.; Zhu, S. P.; Ishihara, K.; Brash, J. L. *Langmuir* **2005**, *21*, 5980–5987.
- (88) Jordan, R.; Ulman, A.; Kang, J. F.; Rafailovich, M. H.; Sokolov, J. *J. Am. Chem. Soc.* **1999**, *121*, 1016–1022.
- (89) Cao, L.; Kruk, M. *Polym. Prepr.* **2008**, *49* (2), 294–295.
- (90) Zhou, F.; Hu, H.; Yu, B.; Osborne, V. L.; Huck, W. T. S.; Liu, W. *Anal. Chem.* **2007**, *79*, 176–182.
- (91) Babin, J.; Lepage, M.; Zhao, Y. *Macromolecules* **2008**, *41*, 1246–1253.
- (92) Huang, J.; Cusick, B.; Pietrasik, J.; Wang, L.; Kowalewski, T.; Lin, Q.; Matyjaszewski, K. *Langmuir* **2007**, *23*, 241–249.
- (93) Pietrasik, J.; Sumerlin, B. S.; Lee, R. Y.; Matyjaszewski, K. *Macromol. Chem. Phys.* **2007**, *208*, 30–36.

MA801643R